RSC Advances

PAPER

View Article Online
View Journal | View Issue

Cite this: *RSC Adv.*, 2020, **10**, 42120

Effect of molecular weight of polyethylene glycol on crystallization behaviors, thermal properties and tensile performance of polylactic acid stereocomplexes

Ruilong Li,[ab] Yifan Wu,[a] Zhuyu Bai,[a] Jianbing Guo[cd] and Xiaolang Chen *[ac]

In this work, the poly(D-lactic acid)–polyethylene glycol–poly(D-lactic acid) (PDLA–PEG–PDLA) triblock copolymer as a novel modification agent was incorporated into poly(L-lactic acid) (PLLA) to improve the thermal and mechanical properties of PLLA. The influences of molecular weight of PEG in the triblock copolymer on the structure, crystallization behaviors, heat resistance and tensile properties of PDLA–PEG–PDLA/PLLA blends were investigated by Fourier transform infrared (FTIR) spectroscopy, X-ray diffraction (XRD), differential scanning calorimetry (DSC), polarized optical microscopy (POM), thermogravimetric analysis (TGA) and tensile testing. The results from FTIR, XRD and DSC confirm the formation of a polylactide stereocomplex in the PLLA blends. The structure and properties of the stereocomplex crystals are different from those of pure PLLA. The melting temperature (T_m) of the stereocrystal is near 200 °C, which is significantly higher than that of the homogeneous crystal of PLLA. The effect of molecular weight of PEG on the crystal morphology of PLLA blends is also obvious. The improvement of tensile properties for PLLA blends is attributed to the crystal morphological features, which will potentially enhance the utility of the PLLA based polymer.

Received 12th October 2020
Accepted 10th November 2020

DOI: 10.1039/d0ra08699a

rsc.li/rsc-advances

1. Introduction

Polymer materials have been widely used in our daily life, but the pollution caused by waste materials is becoming more and more serious.[1,2] Polylactic acid (PLA) has attracted more and more attention because it can be derived from corn stalks and other crops. In addition, PLA finally generates carbon dioxide and water, which does not pollute the environment. Therefore, PLA is regarded as a non-toxic polymer material, and it has a wide range of application in packaging and biomedicine, such as sutures, scaffolds, *et al.*[3–7] According to different monomers, PLA can be divided into poly(L-lactic acid) (PLLA), poly (D-lactic acid) (PDLA) and poly(DL-lactic acid) (PDLLA).[8,9] However, PLA has a very slow crystallization rate, poor toughness, and low heat resistance, which limits its further development and application in some fields.[10–12] Therefore, in order to overcome these disadvantages, the modification of PLA is imperative.

In 1987, Ikada and his co-authors[13] first proposed the PLA stereo structure. It is found that the melting point (T_m) of the co-precipitated mixture of PLLA and PDLA was close to 230 °C,[14] which is 50 °C higher than that of pure PLLA. And X-ray diffraction (XRD) results found that the patterns of the blends were completely different from that of PLLA, exhibiting a new crystalline form. Later this blend was called PLA stereo-complex.[15–17] The crystal structure of PLLA and PDLA is the α crystal form, and the crystal structure of the stereocomplex is a special β crystal form, which belongs to the triclinic lattice and exists in a spiral structure. The unit cell parameter is $a = b =$ 0.916 nm, $c = 0.870$ nm, $\alpha = \beta = 109.2°$, and $\gamma = 109.8°$.[18,19] Sveinbjörnsson *et al.*[20] prepared linear and comb-shaped PLLA and PDLA, and also found that comb-shaped PLLA/linear PDLA blends could form stereo structure. However, the comb-shaped PLLA/comb-shaped PDLA blends mainly form their respective homopolymers. Some scholars also reported the excellent properties of PLA stereocomplex in the subsequent studies.[20,21] Kang and his co-authors[21] also used non-solvent induced phase separation (NIPS) method to obtain PLA stereocomplex/poly(butylene adipate-*co*-terephthalate) (PBAT) bio-scaffold with high properties. This stent has good mechanical properties. For example, the tensile strength increases from 0.3 MPa of pure PLA to 3.8 MPa, and elongation at break also increases slightly. At the same time, the scaffold has a high porosity and can support the attachment and propagation of cells. In

[a]*Key Laboratory of Advanced Materials Technology Ministry of Education, School of Materials Science and Engineering, Southwest Jiaotong University, Chengdu 610031, China. E-mail: chenxl612@sina.com*

[b]*Coal Chemical Industry Technology Research Institute, Ningxia Coal Industry Co. Ltd, China Energy Group, Yinchuan 750411, China*

[c]*Sichuan Jiahe Copoly Technology Co., Ltd., Chengdu 610015, China*

[d]*National Engineering Research Center for Compounding and Modification of Polymer Materials, Guiyang 550014, China*

addition, Gao *et al.*[22] also prepared PLA stereocomplex by melt-blending and extruding at a temperature below the melting point, which inhibited the thermal degradation of PLA. In addition, it is found that the addition of PBAT can promote the formation of stereo crystals. The results show that the addition of 30% PBAT can smooth the surface of the stereocomplex.

The stereo structure also has an obvious influence on the PLA crystallization behaviors. Cui and his co-authors[23] fabricated PLLA/PDLA blends by using polyethylene glycol (PEG) as a plasticizer and TMC-306 as a nucleating agent. Based on the results of XRD patterns and differential scanning calorimetry (DSC) curves, it is not found that the homogeneous crystal is observed after the addition of PEG, TMC-306, or both into the blends. Through non-isothermal and isothermal crystallization kinetics analysis, it is concluded that the half crystallization time of the blends is significantly shortened and the crystallization rate increases with the addition of PEG and TMC-306. Zhou *et al.*[24] synthesized linear PLLA, linear PDLA, star-shaped PLLA and star-shaped PDLA by ring-opening polymerization with 3-butyn-1-ol and pentaerythritol as initiators, respectively. In these blends, the crystallization rate of star-shaped PLLA/PDLA and PLLA/star-shaped PDLA stereocomplex is fast, and the crystallinity is high compared with pure PLLA. This is because the spherulite density of the star chain is large, and the chain mobility of the linear chain is good.

Our group has studied the introduction of PEG in PDLA and synthesis of triblock copolymer of PDLA–PEG–PDLA by ring-opening polymerization.[25] Polarized optical microscopy (POM) showed that PEG shortened the crystallization time of the copolymer and accelerated the crystallization rate. In this work, PDLA–PEG–PDLA triblock copolymers with different molecular weight of PEG were blended with PLLA in solution to fabricate PLA stereocomplex. The effect of the molecular weight of PEG on the crystal structure, crystallization behaviors, heat resistance and mechanical properties of the blends is investigated in detail by using Fourier transform infrared (FTIR) spectroscopy, XRD, DSC, POM, thermogravimetric analysis (TGA), and tensile test. The change of structure was correlated to the enhancement of the thermal and mechanical properties obtained.

2. Experimental

2.1 Materials

PLLA (2002D) was purchased from NatureWorks Company (USA). Dichloromethane (CH_2Cl_2) (AR) was supplied by Chengdu Kelong Chemical Reagent Company (China). The triblock copolymer of PDLA–PEG–PDLA with different molecular weights of PEG (2000, 4000, 6000, and 8000) was synthesized by ring-opening polymerization of D-lactide by using PEG as an initiator and stannous octoate as a catalyst according to our previous study.[25]

2.2 Fabrication of PDLA–PEG–PDLA/PLLA blends

The blends of triblock copolymer and PLLA 2002D were fabricated as following the steps. The solid PDLA–PEG–PDLA triblock copolymer and granular PLLA were accurately weighed and placed in a dry three-necked bottle, and then the dichloromethane solvent was added to the three-necked bottle. Then the three-necked was put in the thermostatic water bath pot at 30 °C for 3 h until the medicine was completely dissolved. The well-stirred solution was poured into the surface dish to evaporate the solvent at room temperature until the sample became film. Finally, the thin-film sample was dried completely in the oven at 80 °C. The ratio of PLLA and PDLA–PEG–PDLA in the blends is fixed at 9 : 1.

2.3 Measurements and characterization

2.3.1 Fourier transform infrared (FTIR) spectra. FTIR spectra of fully dried film of samples were conducted on a Nicolet-6700 FTIR spectrometer after 32 scans within 4000–400 cm^{-1} at a resolution of 2 cm^{-1}.

2.3.2 X-ray diffraction (XRD). The XRD patterns were collected on a powder X-ray diffractometer (PANalytical Netherlands) with Cu-Kα radiation ($\lambda = 0.15418$ nm) at 40 kV and 40 mA. The scanning angle range of X-ray diffractometer is 5–60°.

2.3.3 Differential scanning calorimetry (DSC). DSC thermograms were obtained with a Q20 (TA Instruments, USA). The tests were conducted under nitrogen atmosphere with the flow rate of 50 mL min^{-1}. The specimens were heated from 0 to 250 °C at a heating rate of 10 °C min^{-1}, and the relevant data were recorded.

2.3.4 Polarized optical microscopy (POM). The POM (CX40P, Ningbo Shunyu Instrument Co., Ltd., China) was used to observe the crystal morphologies of pure PLLA and its blends. The samples were first annealed at 220 °C for 5 min, and then quickly cooled to 140 and 180 °C for different crystallization time. Overall crystallization behaviors of samples were also monitored by the digital images.

2.3.5 Thermogravimetric analysis (TGA). TGA curves were conducted by the Q50 thermogravimetric analyzer (TA Instruments, USA) from room temperature to 700 °C under nitrogen atmospheres at a heating rate of 10 °C min^{-1}.

2.3.6 Tensile properties test. Tensile stress–strain behaviors of samples were performed by using a tensile tester (AGS-J, Shimadzu Corporation of Japan) with a crosshead speed 3 mm min^{-1}. All the tests were performed at 23 ± 2 °C. The results were the average values of at least five specimens.

3. Results and discussion

3.1 FTIR of PLA stereocomplex

Fig. 1 shows the FTIR spectra of PLLA, PEG and PDLA–PEG–PDLA/PLLA blends with different molecular weights of PEG. Although the molecular weight of the PEG segments in the blends is different, however, the characteristic peak shapes of four groups of blends with different molecular weight of PEG are basically the same, which also indicates that the molecular weight of PEG has little effect on the FTIR spectra of the blends. The absorption peak around 2991 cm^{-1} in the blends is the stretching vibration peak of CH_3, while the absorption vibration peak of CH_3 in pure PLLA is at 2998 cm^{-1},[26] which indicates that the absorption peak of the CH_3 of the blends is toward the low

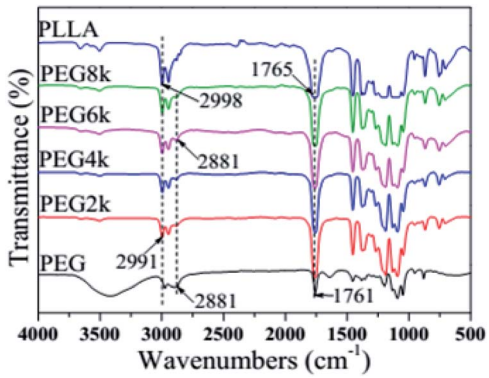

Fig. 1 FTIR spectra of pure PLLA, PEG and PDLA–PEG–PDLA/PLLA blends with different molecular weight of PEG.

wavenumber. Similarly, the stretching vibration peak of C=O in the blends is at 1761 cm^{-1}, and the stretching vibration peak of C=O in pure PLLA is at 1765 cm^{-1}, however, the peak of C=O of the blends moves to the lower position. The absorption peaks of CH_3 and C=O shift to low wavenumbers, which indicates that a hydrogen bond $CH_3\cdots O{=}C$ is formed between the PLLA and PDLA segments. This is a very important feature of the formation of stereocomplex.[27] In addition, a weak absorption peak appears at 2881 cm^{-1} in the spectra of the blends, which is attributed to the stretching vibration peak of CH_2 in PEG, as shown in the curve of PEG spectrum. But this absorption peak is not found in the pure PLLA spectrum, which also proves that the stereocomplex is successfully fabricated.

3.2 Crystal structure of PLA stereocomplex

Fig. 2 shows the XRD patterns of PLLA, PEG and the PLLA blends with different molecular weight of PEG. The (010) and (015) crystal planes of the α crystal form of PLA homopolymer are at $2\theta = 14.7$ and 22.3°, respectively, and the peaks at 16.8 and 19.1° are assigned to the (110)/(200) and (015) crystal planes, respectively.[28,29] In the PDLA–PEG–PDLA triblock copolymer, when the PEG molecular weights are 4000, 6000 and 8000, the diffraction peaks of the stereocrystal for the blends are mostly present. The peaks at 11.8°, 20.6° and 24.1° are assigned to the (110), (300)/(030), and (220) crystal planes of the stereocrystal, respectively.[30,31] Although the diffraction peak of stereocrystals exists when the molecular weight of PEG in triblock copolymer is 2000, the diffraction peaks of homogeneous crystals also appear strongly at 16.8 and 19.1°. This suggests that not only the stereocomplex crystals of PDLA and PLLA but also the homogeneous crystals of PLA exist in the blends when the molecular weight of PEG is low. With increasing the molecular weight of PEG, the homogeneous crystals of PLA disappear. In addition, the diffraction peak intensity of the stereocrystals in the blends tends to increase gradually, and the peak shape becomes much sharper with increasing the molecular weight of PEG in triblock copolymer, which indicates that change of PEG molecular weight has an inducing effect on the formation of stereocrystals. In addition, the higher the molecular weight is, the more obvious the induction effect is. The incorporation of PEG with better molecular chain flexibility as soft block in the triblock copolymer makes the molecular chain of the stereocomplex to be also flexible, so that more stereocrystals can be formed easily. This can also be confirmed in previous work.[32]

3.3 Crystallization and melting behaviors of PLA stereocomplex

Fig. 3 shows the DSC melting curves of pure PLLA, PEG and the PDLA–PEG–PDLA/PLLA blends containing with different molecular weight of PEG, and the corresponding detailed data is listed in Table 1. It is obviously observed from Fig. 3 that the effect of molecular weight of PEG on the melting behaviors of PLLA is very significant. Pure PLLA has an obvious step at 65.8 °C, which is its glass transition. There is no obvious crystal peak, and it is clearly observed from Fig. 3 that the melting temperature (T_m) of PLLA is at 153.6 °C. On the other hand, only one melting peak exists for PEG, and the T_m is at about 62.3 °C. For the DSC curves of the PLLA blends, the melting peak of homogeneous crystal is at about 150 °C, however, there is also a melting peak of stereocrystal at about 200 °C. In addition, the glass transition temperature (T_g) also decreases significantly compared with that of pure PLLA, as listed in Table 1. When the molecular weight of PEG is 6000 or 8000, the value of T_g decreases to about 51 °C, which also indicates that PEG with

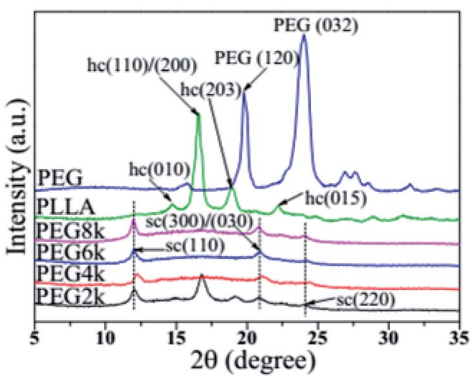

Fig. 2 XRD patterns of pure PLLA, PEG and PDLA–PEG–PDLA/PLLA blends with different molecular weight of PEG.

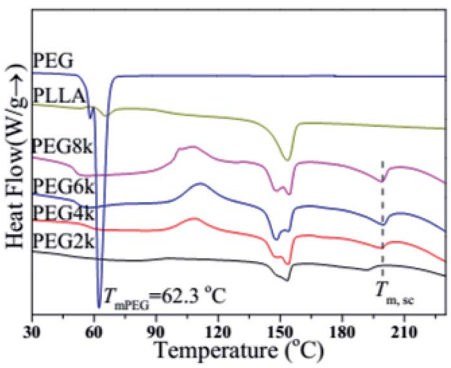

Fig. 3 DSC melting curves of pure PLLA, PEG and PDLA–PEG–PDLA/PLLA blends with different molecular weight of PEG.

Table 1 DSC data of pure PLLA and PDLA–PEG–PDLA/PLLA blends with different molecular weight of PEG

Samples	T_g (°C)	T_{cc} (°C)	ΔH_{cc} (J g^{-1})	$T_{m,hc}$ (°C)	$\Delta H_{m,hc}$ (J g^{-1})	$T_{m,sc}$ (°C)	$\Delta H_{m,sc}$ (J g^{-1})
PLLA	65.8	—	—	153.6	25.0	—	—
PEG2k	—	—	—	153.5	4.8	192.0	1.1
PEG4k	57.4	108.6	7.8	143.4 154.0	13.6	198.7	3.2
PEG6k	51.1	111.3	8.3	148.5 154.3	9.5	199.8	3.3
PEG8k	51.1	106.8	10.7	147.8 154.6	12.2	199.2	4.8

high molecular weight can improve the flexibility of the molecular chain of the blends. When the molecular weight of PEG is 2000, DSC melting curve of the blend is also significantly different from that of the other three-group blends. Its glass transition step has no obvious position on the curve. There is no exothermic peak of cold crystallization, and the T_m of stereocrystal is smaller than the other three groups. The position of the melting peak is not prominent, and the melting enthalpy is also small. With increasing the molecular weight of PEG gradually, there are obvious glass transitions, cold crystallization peaks, homogeneous crystal melting peaks and stereocrystal melting peaks in the DSC melting curves, which indicates that there is a certain amount of stereo crystals in the blends. The T_m of the stereocrystal is at around 200 °C, which is significantly higher than that of the homogeneous crystal. In addition, the melting enthalpy of homogeneous crystals decreases when the molecular weight of PEG is 6000, which indicates that the amount of homogeneous crystals decreases, and the amount of stereocrystals increases in the blends. Additionally, the proportion of high-melting stereocrystals increases. Therefore, heat resistance of the blends is improved due to the formation of stereocrystals.

3.4 Crystal morphological features of PLA stereocomplex

Earlier DSC is used to characterize the melting and crystallization behaviors of the PLA stereocomplex. In order to further understand the crystallization behavior of the PLLA blends, we observed its crystal morphologies at different temperatures and time. Fig. 4 and 5 show the effect of the molecular weight of PEG on the crystal morphological features of the PLLA blends with increasing the crystallization time from 5 min to 4 hours at 140 °C and 180 °C, respectively. It can be clearly seen from Fig. 4 that there is a significant difference in the size and morphological structure of crystals in these samples. The crystallization rate of pure PLLA is very slow when crystallization time is below 1 h, as shown in Fig. 4a. With prolonging the crystallization time, more complete and bigger spherical crystals are formed, which is attributed to the α-crystals of PLLA.[33,34] However, the addition of triblock copolymer with different molecular weight of PEG obviously improves the crystallization rate and changes spherulite structure of PLLA, as shown in Fig. 4b–e. The grain size in the photo is very small, and there is no obvious black cross extinction phenomenon when the crystallization time is short. With increasing crystallization time, it is found that the

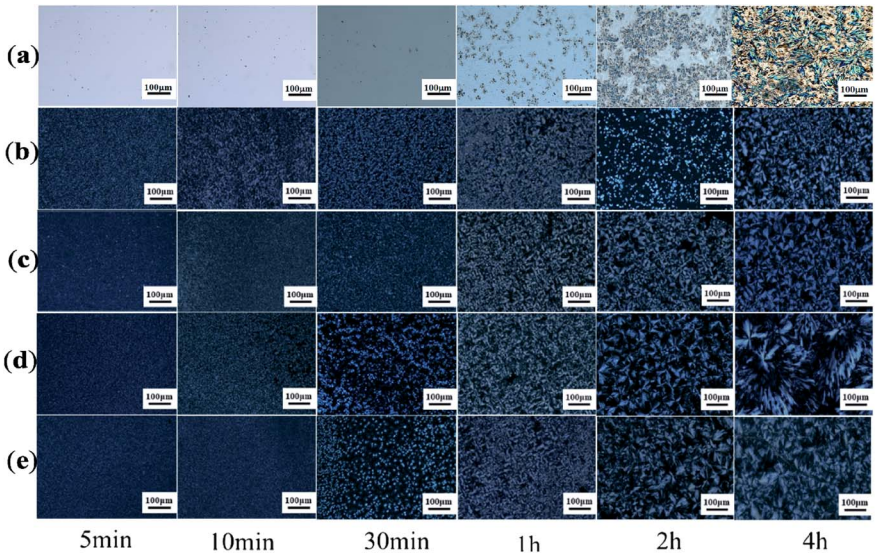

Fig. 4 POM photos of PDLA–PEG–PDLA/PLLA blends with different molecular weight of PEG at 140 °C: (a) pure PLLA; (b) PEG2000; (c) PEG4000; (d) PEG6000; and (e) PEG8000.

crystal size gradually increases. It is concluded from the DSC curves that there are both homogeneous crystals and stereocrystals in the blends at this time, which are mixed crystals. Viewed in the longitudinal direction, with a certain temperature and crystallization time, the size of the PLA crystal also increases with increasing the molecular weight of PEG. However, when the molecular weight of PEG is 8000, the grain size decreases slightly, as shown in Fig. 4e. The grain size reaches the maximum when the molecular weight of PEG is 6000. The increase of the molecular weight of PEG induces the crystallization of PLLA, revealing the improvement of the flexibility of PLLA molecular chain to a certain extent. But when the molecular weight of PEG is too large and exceeds the limit, the PLLA molecular chain becomes too long and is easy to be entangled, which weakens the flexibility and causes resistance to crystallization.

Then we raise the holding temperature to 180 °C, and the crystal at this temperature is basically stereo crystal, as shown in Fig. 5. It is obviously found from Fig. 5 that the nucleation and crystallization are not observed for pure PLLA because the crystallization temperature is higher than the T_m of pure PLLA. Therefore, it is concluded that the morphological features of the blends are attributed to the formation of stereocrystals, as shown in Fig. 5b–e. At the same time, the formation of stereocrystals in the blends is also influenced by the molecular weight of PEG in the triblcok copolymer. When the molecular weight of PEG is 2000, there are only small crystal grains in the early stage of crystallization, especially for 5, 10, and 30 min. However, at the initial stage of crystallization, the grain size also creases gradually with increasing the molecular weight of PEG. When the crystallization time is 4 h, the crystal growth is basically completed. No matter what the molecular weight of PEG is, the obvious black cross extinction phenomenon cannot be observed on the crystal grains. From two groups of different temperature

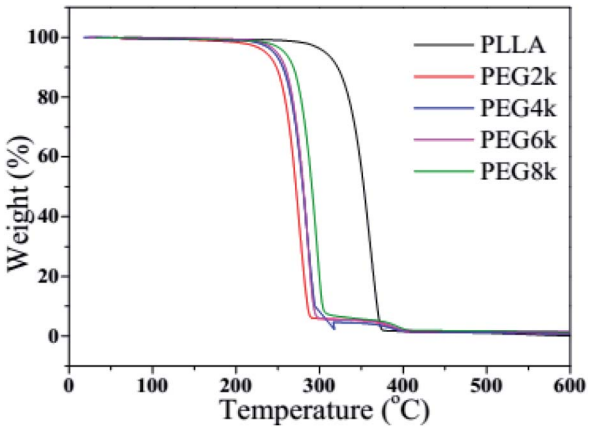

Fig. 6 TGA curves of pure PLLA and PDLA–PEG–PDLA/PLLA blends with different molecular weight of PEG.

polarization microscope photos of comparison, it is concluded that when the PDLA–PEG–PDLA/PLLA blends heat preservation temperature and crystallization time at the same time, the size of the crystallization of the PLLA blends will relatively increase, and the number will increase gradually with increasing the molecular weight of PEG. However, the molecular weight of PEG is too large, which will also bring obstacles to promoting the crystallization of stereocomplex.

3.5 Thermal stability of PLA stereocomplex

Fig. 6 and 7 show the TGA and DTG curves of pure PLLA and PDLA–PEG–PDLA/PLLA blends with different molecular weight of PEG, respectively, and the detailed data is also listed in Table 2. It is clearly observed from Fig. 6 and 7 that the thermal degradation process of pure PLLA shows one-step degradation. It can be found from Table 2 that the temperature of 10% weight

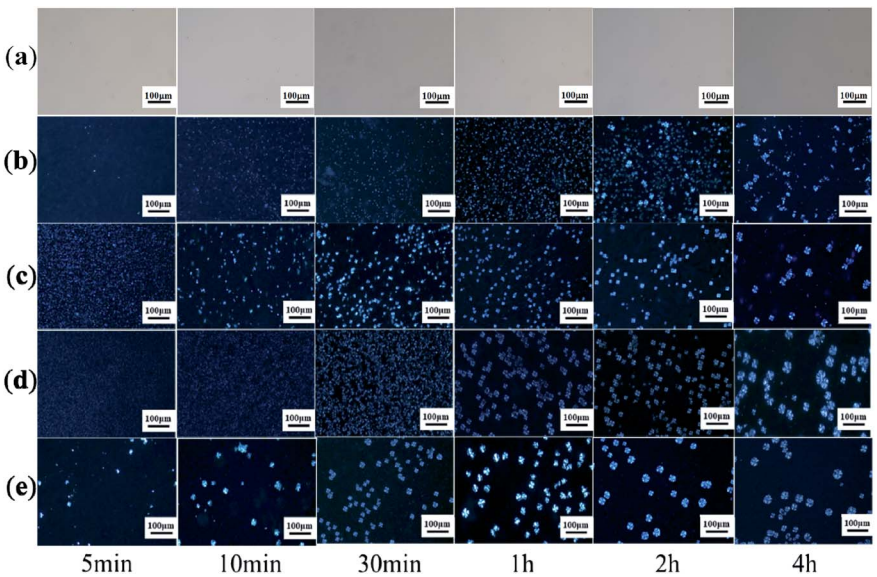

Fig. 5 POM photos of PDLA–PEG–PDLA/PLLA blends with different molecular weight of PEG at 180 °C: (a) pure PLLA; (b) PEG2000; (c) PEG4000; (d) PEG6000; and (e) PEG8000.

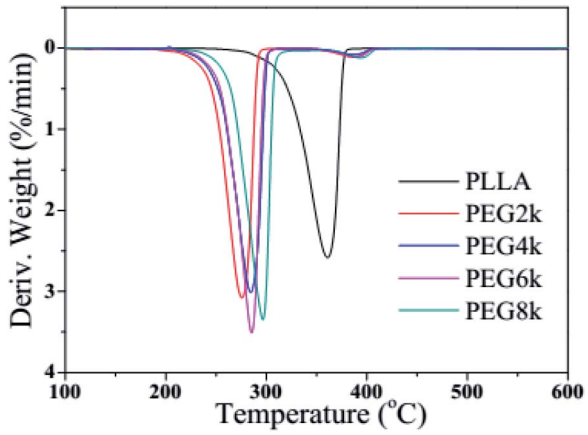

Fig. 7 DTG curves of pure PLLA and PDLA–PEG–PDLA/PLLA blends with different molecular weight of PEG.

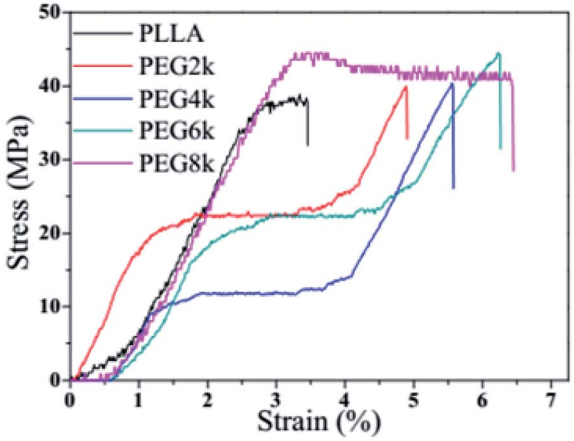

Fig. 8 Tensile stress and strain curves of pure PLLA and PDLA–PEG–PDLA/PLLA blends with different molecular weight of PEG.

Table 2 TGA data of pure PLLA and PDLA–PEG–PDLA/PLLA blends with different molecular weight of PEG[a]

Samples	$T_{10\%}$ (°C)	$T_{30\%}$ (°C)	$T_{50\%}$ (°C)	T_{peak} (°C)
PLLA	321.4	342.4	352.7	361.0
PEG2k	248.3	263.7	271.5	275.6
PEG4k	255.8	271.6	279.8	284.4
PEG6k	258.7	272.7	280.4	285.3
PEG8k	268.5	282.8	290.6	296.5

[a] $T_{10\%}$, $T_{30\%}$, $T_{50\%}$ represent the mass loss 10%, 30%, 50% rate of the temperature; T_{peak} represents the maximum mass loss rate of temperature.

Table 3 Elongation at break and tensile strength of pure PLLA and PDLA–PEG–PDLA/PLLA blends with different molecular weight of PEG

Samples	Elongation at break (%)	Tensile strength (MPa)
PLLA	3.5 ± 0.2	38.4 ± 0.4
PEG2k	4.9 ± 0.1	39.7 ± 0.5
PEG4k	5.6 ± 0.2	40.4 ± 0.4
PEG6k	6.3 ± 0.3	44.5 ± 0.3
PEG8k	6.5 ± 0.1	44.4 ± 0.5

loss of PLLA is 321.4 °C, and the mass loss is 30% when the temperature reaches 342.4 °C. The mass loss rate reaches the maximum when the temperature arrives at 361.0 °C. It is reported that PEG begins to degrade at less than 200 °C.[35] It can be observed from Fig. 6 and Table 2 that the initial decomposition temperature of the blends decreases with the addition of PDLA–PEG–PDLA triblock copolymer, and there is a two-step decomposition behavior. The first step of degradation is mainly attributed to the decomposition of PEG, and the second step of degradation is attributed to the decomposition of the stereocrystals in the PLLA blends. With increasing the molecular weight of PEG in the triblock copolymer, the initial decomposition temperature of the blends also increases, and the span from the initial decomposition temperature to the complete decomposition temperature increases, indicating that the heat resistance of the PLA stereocomplex is in a positive direction development.

3.6 Tensile properties of PLA stereocomplex

Tensile stress–strain curves of PLLA and PDLA–PEG–PDLA/PLLA blends with different molecular weights of PEG are shown in Fig. 8, and the specific data are also listed in Table 3. The tensile strength and elongation at break of pure PLLA is 38.4 MPa, and 3.5%, respectively. After the triblock copolymer is added into PLLA matrix, the dramatic improvements in tensile strength and elongation at break observed for these blends are shown in Fig. 8 and Table 3. This is attributed to the formation of the stereo structure in the PLLA blends. It is observed that the stress at break, toughness, and elongation at break of the blends containing only 10% triblock increase gradually with increasing the molecular weight of PEG. For example, when the molecular weight of PEG is 2000, the tensile strength and elongation at break of the blends are 39.7 MPa and 4.9%, respectively. When the molecular weight of PEG increases to 8000, however, the tensile strength and elongation at break of the blends increase to 44.4 MPa and 6.5%, respectively. On the one hand, with increasing molecular weight of PEG, the chain entanglement will increase, which will inhibit the relative slip of PLLA fiber. On the other hand, the side arms of the triblock copolymer form stereocomplex with PLA which nucleates crystallization of PLLA matrix in the PLLA blends. At the same time, the soft midblock of the triblock copolymer is trapped within the semicrystalline polymer thus forming a multiphase structure consisting of hard domains dispersed in a continuous amorphous phase. All these play an important role in improving the mechanical properties of PLLA matrix.

4. Conclusions

The PDLA–PEG–PDLA/PLLA blends are prepared by the introduction of PDLA–PEG–PDLA triblock copolymer containing

different molecular weight of PEG into PLLA matrix. The results of FTIR and XRD indicate that the PLA stereocomplex is successfully constructed. When the molecular weight of PEG in the tribolck copolymer is low, the content of homogeneous crystals in the stereocomplex is high. However, the stereocrystals in the blends account for the majority with increasing the molecular weight of PEG. The DSC results show that the T_m value of the stereocrystal in the blends is around 200 °C, which is much higher than that of the homogeneous crystal of PLLA, and the heat resistance is improved significantly. The crystals and crystallization morphology of the blends are obviously affected by the crystallization temperature and time. Both the homogeneous crystals and stereocrystals exist in the blends at 140 °C, however, only stereocrystals can be observed in the blends at 180 °C. In addition, the grain size increases and then decreases with increasing the molecular weight of PEG. In addition, the formation of stereocrystals in the blends is also affected by the molecular weight of PEG in the triblcok copolymer. Additional investigations on the crystallization morphologies of the blends also provide a better understanding of the improvement of mechanical properties. Use of longer soft blocks of PEG in the tribolck copolymer provides an opportunity for further enhancing the tensile strength and elongation at break of PLLA matrix.

Conflicts of interest

The authors declare that they have no known competing financial interests or personal relationships that could have appeared to influence the work reported in this paper.

Acknowledgements

The authors gratefully acknowledge the research funding provided by International Science and Technology Cooperation Project of Sichuan (2019YFH0047), International Science and Technology Cooperation Project of Chengdu (2020-GH02-00010-HZ), Opening Project of State Key Laboratory of Polymer Materials Engineering (Sichuan University) (2017-4-02), and Science and Technology Project Foundation of Guizhou (2016/5667, 2017/5788).

References

1 C. A. Ramírez-Herrera, A. Flores-Vela, A. M. Torres-Huerta and M. A. Domínguez-Crespo, PLA degradation pathway obtained from direct polycondensation of 2-hydroxypropanoic acid using different chain extenders, *J. Mater. Sci.*, 2018, **53**, 10846–10871.

2 M. A. Elsawy, K. H. Kim, J. W. Park and A. Deep, Hydrolytic degradation of polylactic acid (PLA) and its composites, *Renewable Sustainable Energy Rev.*, 2017, **79**, 1346–1352.

3 B. Tyler, D. Gullotti, A. Mangraviti, T. Utsuki and H. Brem, Polylactic acid (PLA) controlled delivery carriers for biomedical applications, *Adv. Drug Delivery Rev.*, 2016, **107**, 163–175.

4 Z. Sheikh, S. Najeeb, Z. Khurshid, V. Verma, H. Rashid and M. Glogauer, Biodegradable materials for bone repair and tissue engineering applications, *Materials*, 2015, **8**, 5744–5794.

5 D. Kai, W. Ren, L. L. Tian, P. L. Chee, Y. Liu, S. Ramakrishna and X. J. Loh, Engineering poly(lactide)-lignin nanofibers with antioxidant activity for biomedical application, *ACS Sustainable Chem. Eng.*, 2016, **4**, 5268–5276.

6 M. Oliveira, E. Santos, A. Araújo, G. J. M. Fechine, A. V. Machado and G. Botelho, The role of shear and stabilizer on PLA degradation, *Polym. Test.*, 2016, **51**, 109–116.

7 R. M. Rasal, A. V. Janorkar and D. E. Hirt, Poly(lactic acid) modifications, *Prog. Polym. Sci.*, 2010, **35**, 338–356.

8 H. Tsuji and Y. Ikada, Blends of crystalline and amorphous poly(lactide). 3. Hydrolysis of solution-cast blend films, *J. Appl. Polym. Sci.*, 2015, **63**, 855–863.

9 M. S. Lopes, A. L. Jardini and R. Maciel, Poly (lactic acid) production for tissue engineering applications, *Procedia Eng.*, 2012, **42**, 1402–1413.

10 A. R. Kolahchi and M. Kontopoulou, Chain extended poly(3-hydroxybutyrate) with improved rheological properties and thermal stability, through reactive modification in the melt state, *Polym. Degrad. Stab.*, 2015, **121**, 222–229.

11 X. Y. Hu, T. T. Su, P. Li and Z. Y. Wang, Blending modification of PBS/PLA and its enzymatic degradation, *Polym. Bull.*, 2018, **75**, 533–546.

12 J. H. Guo, J. X. Qiao and X. Zhang, Effect of an alkalized-modified halloysite on PLA crystallization, morphology, mechanical, and thermal properties of PLA/halloysite nanocomposites, *J. Appl. Polym. Sci.*, 2016, **48**, 133.

13 Y. Ikada, K. Jamshidi, H. Tsuji and S. H. Hyon, Stereocomplex formation between enantiomeric poly(lactides), *Macromolecules*, 1987, **20**, 904–906.

14 Y. H. Jing, C. Y. Quan, B. Liu, Q. Jiang and C. Zhang, A mini review on the functional biomaterials based on poly(lactic acid) stereocomplex, *Polym. Rev.*, 2016, **56**, 262–286.

15 H. Tsuji, S. H. Hyon and Y. Ikada, Stereocomplex formation between enantiomeric poly(lactic acid)s. 3. Calorimetric studies on blend films cast from dilute solution, *Macromolecules*, 1991, **24**, 5651–5656.

16 V. Arias, K. Odelius, A. Höglund and A. C. Albertsson, Homocomposites of polylactide (PLA) with induced interfacial stereocomplex crystallites, *ACS Sustainable Chem. Eng.*, 2015, **39**, 2220–2231.

17 P. Barbosa, J. Campos, A. Turygin, V. Y. Shur, A. Kholkin, A. B. Timmons and F. M. Figueiredo, Piezoelectric poly(lactide) stereocomplexes with a cholinium organic ionic plastic crystal, *J. Mater. Chem. C*, 2017, **5**, 12134–12142.

18 T. Okihara, M. Tsuji, A. Kawaguchi, K. I. Katayama, H. Tsuji, S. H. Hyon and Y. Ikada, Crystal structure of stereocomplex of poly(L-lactide) and poly(D-lactide), *J. Macromol. Sci., Part B: Phys.*, 1991, **30**, 119–140.

19 W. Liu, S. C. He and Y. J. Yang, Effect of stereocomplex crystal on foaming behavior and sintering of poly(lactic acid) bead foams, *Polym. Int.*, 2012, **8**, 516–526.

20 B. R. Sveinbjörnsson, G. M. Miyake, A. El-Batta and R. H. Grubbs, Stereocomplex formation of densely grafted brush polymers, *ACS Macro Lett.*, 2014, **3**, 26–29.
21 Y. Kang, P. Chen, X. T. Shi, G. C. Zhang and C. Y. Wang, Preparation of open-porous stereocomplex PLA/PBAT scaffolds and correlation between their morphology, mechanical behavior, and cell compatibility, *RSC Adv.*, 2018, **82**, 12933–12943.
22 X. R. Gao, B. Niu, W. Q. Hua, Y. Li, L. Xu, Y. Wang, X. Ji, G. J. Zhong and Z. M. Li, Rapid preparation and continuous processing of polylactide stereocomplex crystallite below its melting point, *Polym. Bull.*, 2019, **76**, 3371–3385.
23 L. Cui, Y. H. Wang, Y. Guo, Y. Liu, J. C. Zhao, C. J. Zhang and P. Zhu, Cooperative effects of nucleation agent and plasticizer on crystallization properties of stereocomplex-type poly(lactide acid), *Polym. Adv. Technol.*, 2016, **37**, 1301–1307.
24 K. Y. Zhou, J. B. Li, H. X. Wang and J. Ren, Effect of star-shaped chain architectures on the polylactide stereocomplex crystallization behaviors, *Chin. J. Polym. Sci.*, 2017, **35**, 974–991.
25 Y. F. Wu, L. T. Li, S. P. Chen, J. Qin, X. L. Chen, D. F. Zhou and H. Wu, Synthesis, characterization, and crystallization behaviors of poly(D-lactic acid)-based triblock copolymer, *Sci. Rep.*, 2020, **10**, 3627.
26 G. Kister, G. Cassanas and M. Vert, Effects of morphology, conformation and configuration on the IR and Raman spectra of various poly(lactic acid)s, *Polymer*, 1998, **39**, 267–273.
27 A. Gupta, A. K. Pal, E. M. Woo and V. Katiyar, Effects of amphiphilic chitosan on stereocomplexation and properties of poly(lactic acid) nano-biocomposite, *Sci. Rep.*, 2018, **8**, 4351.
28 S. H. Im, Y. Jung and S. H. Kim, In situ homologous polymerization of l-lactide Having a stereocomplex crystal, *Macromolecules*, 2018, **51**, 6303–6311.
29 N. Ji, G. Hu, J. B. Li and J. Ren, Influence of poly(lactide) stereocomplexes as nucleating agents on the crystallization behavior of poly(lactide)s, *RSC Adv.*, 2019, **9**, 221–6227.
30 D. Pholharn, Y. Srithep and J. Morris, Melt compounding and characterization of poly(lactide) stereocomplex/natural rubber composites, *Polym. Eng. Sci.*, 2018, **5**, 713–718.
31 Z. X. Jing, X. T. Shi, G. C. Zhang and J. Li, Rheology and crystallization behavior of PLLA/TiO2-g-PDLA composites, *Polym. Adv. Technol.*, 2015, **26**, 528–537.
32 F. Qi, M. Q. Tang, X. L. Chen, M. Chen, Y. H. Ma, G. Guo, Z. B. Zhang and W. D. He, Morphological structure, thermal and mechanical properties of tough poly(l-lactide) upon stereocomplexes, *Eur. Polym. J.*, 2015, **71**, 314–324.
33 H. Tsuji, Poly(lactic acid) stereocomplexs: A decade of progress, *Adv. Drug Delivery Rev.*, 2016, **107**, 97–135.
34 V. Arias, K. Odelius, A. Höglund and A. C. Albertsson, Homocomposites of polylactide (PLA) with induced interfacial stereocomplex crystallites, *ACS Sustainable Chem. Eng.*, 2015, **3**, 2220–2231.
35 X. J. Gong, D. Shi, H. H. Zeng, Y. K. Yang, T. Jiang, Q. C. Zhang, S. C. Jiang, R. K. Y. Li and Y. W. Mai, Facile one pot polycondensation method to synthesize the crosslinked polyethylene glycol-based copolymer electrolytes, *Macromol. Chem. Phys.*, 2016, **27**, 1607–1613.